THE JOURNAL OF PHYSICAL CHEMISTRY A

pubs.acs.org/JPCA Article

Conformer Specific Excited-State Structure of 3-Methylthioanisole

Heesung Lee, So-Yeon Kim, Jean Sun Lim, Junggil Kim, and Sang Kyu Kim*

Cite This: https://dx.doi.org/10.1021/acs.jpca.0c03452 Read Online

ACCESS | Metrics & More | Article Recommendations | Supporting Information

ABSTRACT: *Trans* and *cis* conformers of 3-methylthioanisole have been spectroscopically investigated to reveal the conformer specific structural changes upon the $S_1(\pi\pi^*)-S_0$ excitation. The conformational cooling during the supersonic expansion is found to be quite efficient in the Ar carrier gas giving the *trans* conformational isomer exclusively in the molecular beam, whereas both *trans* and *cis* conformers are populated in the jet when the sample is carried in Ne. Using the Stark deflector, *trans* and *cis* conformers are unambiguously identified, showing the distinct Stark deflection profiles according to their sufficiently different dipole moments of 1.013 or 1.670 D, respectively. For the *trans* conformer, the methyl moiety on the *meta*-position adopting the eclipsed geometry in S_0 transforms into the staggered geometry in S_1 to activate a series of the CH_3 torsional mode. A Hamiltonian with the one-dimensional sinusoidal torsional potential is solved using the free-rotor basis set to explain the experiment, giving the 3-fold torsional barrier of 34 and 304 cm^{-1} for S_0 and S_1, respectively. For the *cis* conformer, on the other hand, the CH_3 torsion is little activated in the S_1-S_0 transition as both S_0 and S_1 adopt the staggered geometry at the minimum energy points. The doublet of each band of the *cis* conformer is ascribed to tunneling split due to the very low CH_3 torsional barrier of 27 cm^{-1} in S_0. It is found that the *cis* conformer undergoes a planar to pseudoplanar structural change upon the S_1-S_0 transition. Theoretical calculation based on the double-well model potential curve could explain the experiment quite well, suggesting that the SCH_3 moiety of the *cis* conformer in S_1 becomes out-of-plane with respect to the plane of the phenyl moiety. This implies that excited-state predissociation dynamics of *trans* and *cis* conformers of the title molecule might be different.

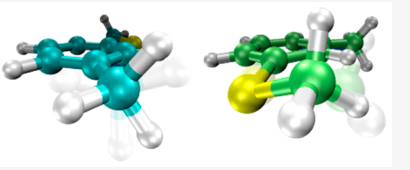

INTRODUCTION

The effect of methylation on electronic structure and reaction dynamics has been one of the central subjects in organic syntheses or biological chemistry as methylation is one of the most important epigenetic processes. From the physical chemist's viewpoint, methylation has been utilized as a great tool for the investigation of intramolecular vibrational redistribution (IVR) dynamics. For instance, methylation on a benzene ring gives rise to the much accelerated IVR process as the CH_3 moiety rotates nearly freely around the H_3C-C bond axis.[1−3] IVR dynamics, especially for the excited-state molecular system, is very important as it tends to delocalize the given energy over the entire nuclear framework of the molecular system. Even though it hampers the design of the bond-selective chemistry, IVR helps the molecule to protect its integrity against external perturbations such as high energy radiation or thermal waves. Namely, the efficient and fast IVR could be quite essential for the system to maintain its chemical and/or biological activities in harsh environments. As a model system for the investigation of IVR dynamics, therefore, spectroscopy[4−8] and dynamics of a variety of methylated molecular systems have been extensively and intensively studied to date. As there are already many excellent review articles on IVR,[9−11] we will rather focus on the title molecule instead of mentioning previous other examples.

Thioanisole has been intensively investigated in recent years.[12−18] As the conical intersections are encountered along the $\pi\pi^*$-mediated $S-CH_3$ bond predissociation dynamics, thioanisole has served as an ideal model system for disentangling complicated nonadiabatic chemistry happening in the proximity of or remote from the conical intersection seam. Particularly, it has been found that the subtle changes of excited-state molecular structures given by the specific S_1-S_0 vibronic transitions dictate the reaction pathway along either the adiabatic or nonadiabatic channel in terms of the product yields and reaction rates,[14] from which one can infer the structure and dynamic property of the conical intersection. Whereas a number of vibronic transitions could be utilized for the exploration of the molecular structures associated with the multidimensional conical intersection seam, one could also employ chemical substitution to modify and engineer the molecular structure especially because the optical transition is often limited by the Franck−Condon (FC) overlap. As a typical example, the 2-fluorothioanisole molecule undergoes an apparent structural change from planar to nonplanar geometry upon the S_1-S_0 optical transition in contrast to the case of thioanisole of which the structure remains planar in both S_1 and S_0.[18] The nonplanar geometry of the S_1 2-fluorothioanisole has been found to lead to a quite different dynamic behavior

Received: April 18, 2020
Revised: May 12, 2020
Published: May 13, 2020

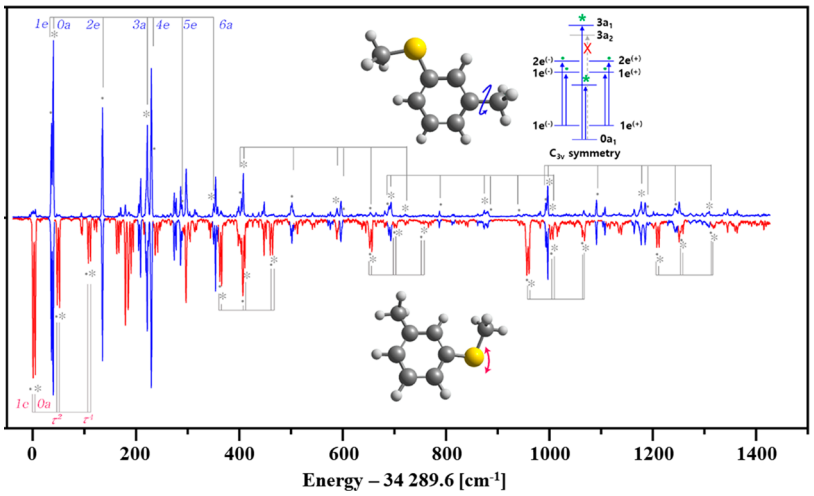

Figure 1. R2PI spectrum of 3-methylthioanisole obtained in (upper) Ar carrier gas with a backing pressure of 1 atm or in (lower) Ne carrier gas with a backing pressure of 3 atm, respectively. Transitions of *trans* (blue) and *cis* (red) conformers are clearly distinct. The progression bands of the methyl internal rotor are activated as denoted in the upper trace. The torsional series is well identified with symmetry species in C_{3V}. According to the hole-burning spectroscopy (see Supporting Information) the e−e (denoted as dots) and a−a (denoted as asterisks) transitions have been unambiguously identified. For the *cis* conformer (lower trace), the out-of-plane dihedral torsional mode of the methylthio (SCH_3) moiety is strongly activated. The doublet is due to the a″−e″ tunneling split through the very low CH_3 torsional barrier in the S_0 *cis*. In the inset, calculated (RICC2, aug-cc-pVDZ) minimum S_1 energy structures of two conformers are shown with arrows corresponding to the geometrical change upon the S_1−S_0 optical transition. The energetic diagram illustrates the symmetry conservation for the C_{3v} methyl internal rotation. The 0_0^0 origin (1e′−1e″) transition energies are found to be 34 289.6 cm^{-1} (*cis*) and 34 325.7 cm^{-1} (*trans*).

along the S-CH_3 predissociation reaction pathway, avoiding the surface crossing near the asymptotic limit. In this regard, it is a natural question whether or not the methylation of thioanisole influences the excited-state reaction dynamics, especially as the nonadiabatic dynamics is so sensitive to the detailed molecular structures.

Herein, we have found that the 3-methylthioanisole (3-MTA) in two distinct conformational structures of *cis* and *trans* shows rich spectroscopic features, revealing the structural change of each conformational isomer upon the S_1−S_0 optical excitation.

The *trans* conformer undergoes the eclipsed-to-staggered geometrical change upon the S_1−S_0 transition as long as the relative orientation of the CH_3 moiety with respect to the SCH_3 moiety is concerned. On the other hand, the *cis* conformer shows little change in the CH_3 torsional geometry as it remains in the staggered form even in S_1. However, the SCH_3 moiety becomes out-of-plane in S_1 of the *cis* conformer. Theoretical calculations based on the simple one-dimensional potential energy function explains the experiment quite well.

EXPERIMENTAL METHODS

The experimental setup was described in a previous work.[16−18] The 3-MTA was purchased (MediGen; >99% purity) and used without further purification. The sample was heated to 75° to be mixed with the Ne or Ar carrier gas. The supersonic jet was produced by the expansion of the gas mixture through a nozzle orifice with a diameter of 0.5 mm (General valve Series 9), followed by a skimmer. The Nd:YAG laser (Surelite II-10, Continuum) was used to pump a dye laser (Lumonics, HD-500) to generate the UV laser pulse in the 280.5−292 nm region by frequency doubling through a beta barium borate (BBO) crystal. The parent ion signal was detected by a position sensitive detector equipped with microchannel plates (MCP), (Burle, ϕ = 40 mm), and phosphor. The Stark-deflector setup had been described previously.[21] For the UV−UV hole burning spectroscopy, another Nd:YAG + dye laser setup was used to produce the laser pulse in the 280.5−292 nm region. The delay time between the laser pulses for hole-burning and probing was set to be 200 ns. Experimental deflection profiles were compared to the simulated profiles using the CMIfly code.[22] Monte Carlo particle sampling was used up to J = 18 with 300 particles per each (J, Ka, Kc, M) state. Stark shift was allowed up to J = 30. Rotational temperature was fixed at 6 K. Rotational constants and dipole moments calculated using the Becke, 3-parameter, Lee-Yang-Parr (B3LYP) functional with the 6-311++G(3df,3pd) basis set was used in the CMIstark program.[23] The CMIfly code was used to record the verticality (molecular position shift) with the time step of 1 μs. The molecular beam velocity along the *z*-axis (beam propagation direction) was fixed, whereas its dispersion along the *x* and *y* axes was derived from the fit to the experiment. Only half of the populations per each quantum state could reach the detection region.

For the calculation of the potential energy curves along the methyl internal rotation and the methylthio group out-of-plane torsion, the second-order coupled cluster model which employs the resolution of the identity approximation (RICC2) was used in the Turbomole 7.0 program.[20] After the simple calculation from the Gaussian 09[19] program with the B3LYP method and the 6-311++G(3df,3pd) basis set for the purpose of initial evaluation, the RICC2 calculations with the aug-cc-pVDZ basis set were performed for the S_0 geometry optimization and harmonic frequency calculations of *trans*- and *cis*-3-methylthioanisole conformers. From the minimum energy structure, the potential energy curves were obtained by the relaxed scan where the dihedral (or CH_3 group torsional) angle of the methylthio group with respect to the molecular plane was fixed while all other degrees of freedom were optimized. Calculated reduced mass for the low-frequency out-of-plane vibration was used in a double-well FC simulation of the *cis* conformer.

https://dx.doi.org/10.1021/acs.jpca.0c03452
J. Phys. Chem. A XXXX, XXX, XXX−XXX

RESULTS AND DISCUSSION

The resonant (1 + 1) two-photon ionization (R2PI) spectrum of the jet-cooled 3-MTA in the Ar or Ne carrier gas is shown in Figure 1, respectively. Interestingly, it has been found that only one conformational species is rather exclusively populated in the Ar jet, whereas both conformers are found to be almost equally probable in the Ne jet. The conformer surviving in the Ar carrier gas is identified as the *trans*-3-MTA (*vide infra*). Naturally, it seems to be that the *trans* conformer is more stable than the *cis* conformer (DFT: 25 cm^{-1}, RICC2:3 cm^{-1}). The conformational cooling is then most efficient in the collisional cooling process with Ar in front of the nozzle orifice. For a more definite identification of the conformer species, the Stark deflector has been employed to get the deflection profiles of two species in the strong electric field using the distinct S_1-S_0 spectral origins of two conformers in the Ne jet. We could definitely identify the *cis* or *trans* conformer as the former is deflected more than the latter according to their distinct dipole moments of 1.67 or 1.013 D, respectively, Figure 2. Stark

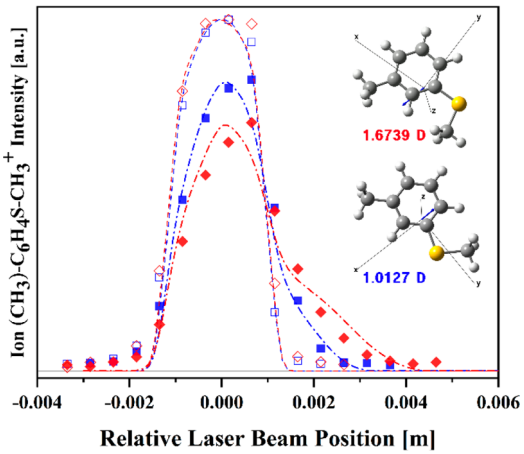

Figure 2. Normalized Stark-deflection profiles obtained for the 0a′−0a″ transitions of (blue) *trans* (34 329 cm^{-1}) and (red) *cis* (34 294.6 cm^{-1}) conformers. Open or filled rectangles represent experimental data at the applied electric field (**E**) of zero or 80 kV/cm, respectively. Dashed (**E** = 0) and dashed-dotted (**E** = 80 kV/cm) lines are simulations (see the text for details). The *cis* conformer (red) shows the more deflected profile compared to the *trans* conformer (blue). Inset molecules are calculated (G09 B3LYP, 6-311++G(3df,3pd)) as minimum energy S_0 structures with their permanent dipole moments.

deflection profiles of both conformers could be simulated quite well. Accordingly, one series of R2PI bands based on the S_1-S_0 origin of 34 289.6 cm^{-1} is attributed to the *cis* conformer, whereas the other R2PI signals starting from the origin of 34 325.7 cm^{-1} belong to the *trans* conformer.

The spectral features of two different conformers are very different from each other. For the *trans* conformer, a series of the CH_3 torsional mode stands out quite obviously. Since the torsional motion of the CH_3 moiety, when its barrier is low, belongs to G6 which is isomorphic to C_{3V}, the symmetry species of the associated eigenstates are classified according to the symmetry elements in the C_{3V} point group. In the S_1-S_0 transition, the symmetry in C_{3V} is conserved as far as the CH_3 torsional mode is concerned. Here, we set a one-dimensional Hamiltonian for the CH_3 rotor based on the sinusoidal model potential as

$$H = -F\frac{\partial^2}{\partial\phi^2} + V(\phi)$$

$$V(\phi) = \sum_n \frac{1}{2}V_n(1 - \cos n\phi)$$

$$V(\phi) = \frac{1}{2}[V_3(1 - \cos 3\phi) + V_6(1 - \cos 6\phi)]$$

Here F is the reduced internal rotational constant for the hindered rotor around the CH_3 torsional angle (ϕ). $V(\phi)$ is the one-dimensional potential energy function where V_3 or V_6 is the 3-fold or 6-fold sinusoidal barrier, respectively. The 31 × 31 Hamiltonian matrix based on the free rotor basis set is then solved to give eigenvalues and eigenfunctions for individual CH_3 torsional modes. The spectrum could be perfectly reproduced when F = 5.34 (or 5.33) cm^{-1}, V_3 = 34 (or 304) cm^{-1}, and V_6 = −25.4 (or −10) cm^{-1} for S_0 (or S_1). The torsional barrier in S_0 is very low, giving rise to the tunneling split of 3.8 cm^{-1} which is responsible for the doublet features of many S_1-S_0 vibronic bands. In S_1, the 3-fold CH_3 torsional barrier is greatly increased to 304 cm^{-1} as above, and corresponding eigenvalues reproduce the experiment very well (Figure 3). Especially, as the eclipsed geometry of CH_3 undergoes the structural change to the staggered geometry, a series of the CH_3 torsional mode is found to be significantly activated. Using the simple FC overlap calculation based on the relation of FC = $|\langle\psi_{S_0}(\phi + \alpha)\,|\,\psi_{S_1}(\phi)\rangle|^2$, it is found that the CH_3 torsional angle at the minimum energy in S_1 is rotated by $\alpha \sim 58°$ from that in S_0, which is compatible with the *ab initio* value (57.9°). It is found that the C_{3V} symmetry of each level is strictly conserved during the S_1-S_0 transition as demonstrated by the hole-burning spectroscopy, Figure 3. While the peak positions and relative intensities of CH_3 torsional bands are well reproduced by the simulation, the assignment for the 193 cm^{-1} band is not straightforward yet. One may be tempted to assign this band as the 4e′−1e″ transition, but it is less likely as the experiment shows the clear depletion of the 193 cm^{-1} band upon the hole-burning of the 0a′−0a″ transition.

Namely, since the hole-burning behavior strongly indicates that the 193 cm^{-1} band originates from the 0a″ level in S_0, unless the symmetry is broken, it is hardly assignable to one of the CH_3 torsional modes. One possibility would be then that the 193 cm^{-1} band is the consequence from the coupling of the CH_3 torsional 4e′ mode to another otherwise optically dark nearly degenerate mode. The other possibility is that the restriction given by the symmetry conservation among C_{3V} symmetry species is loosened for eigenfunctions located near the top of the torsional barrier, although symmetry breaking for the optical transitions among the CH_3 rotor levels has rarely been reported.[7,8] The nature of this band is definitely subject to the further investigation. We have found additional series of the CH_3 rotor bands combined with many other vibrational modes, Figure 1. As the *trans*-3-MTA undergoes a substantial geometrical change, the CH_3 torsional mode is found to be highly activated for all Franck−Condon active modes. Mode assignments are given in the Supporting Information (Table S1) with well-matched theoretical values.

For the *cis* conformer, there is little geometrical change upon the S_1-S_0 transition in terms of the CH_3 rotation with respect to the molecular plane. Namely, the staggered geometry in S_0 remains the same also in S_1. The doublet feature of each band is clearly observed in the R2PI spectrum of *cis*, giving the split

https://dx.doi.org/10.1021/acs.jpca.0c03452
J. Phys. Chem. A XXXX, XXX, XXX−XXX

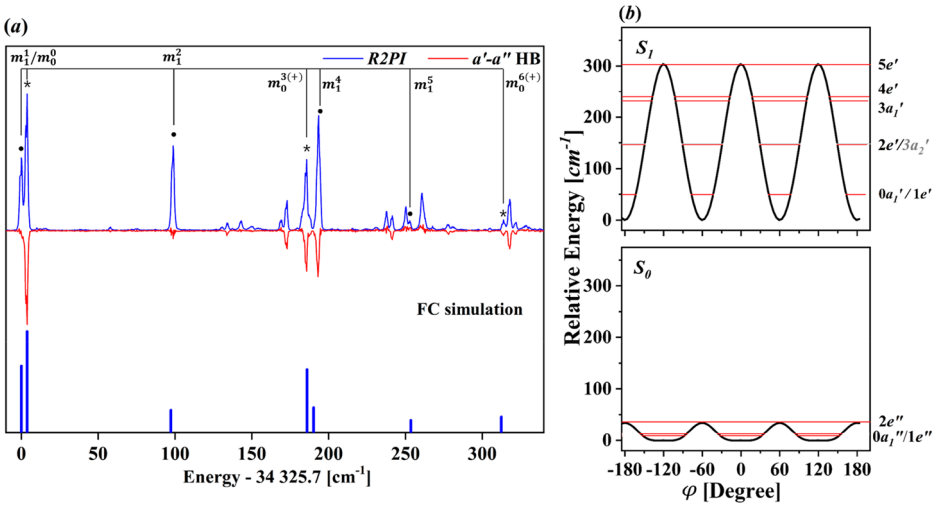

Figure 3. (a) R2PI spectrum of the *trans* 3-MTA obtained with the Ar carrier gas (upper blue solid line). The hole-burning spectrum after the depletion through the 0a′−0a″ transition is shown just below as a red solid line. The simulated stick spectrum (lower trace) is obtained from the FC simulation (see the text). Dots and asterisks are denoted for "e" and "a" symmetry species of the CH_3 internal rotor, respectively. The hindered rotor transitions are depicted according to the internal rotor quantum numbers (m) of S_0 (subscript) and S_1 (superscript). (b) The sinusoidal model potential energy curves for the CH_3 internal rotor in S_0 and S_1 where φ is the rotational angle of the CH_3 about the C−C axis. Eigenvalues and associated symmetry species are also shown.

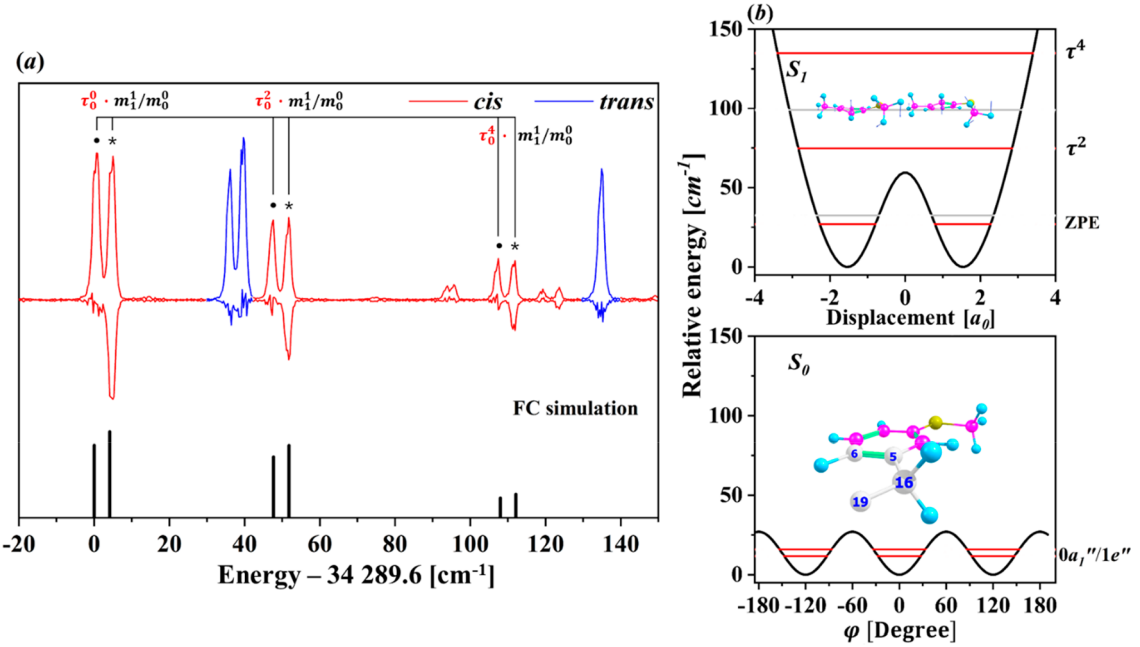

Figure 4. (a) R2PI spectrum of the *cis* 3-MTA (red) obtained with the Ne carrier gas (upper red solid line). The hole-burning spectrum after the depletion through the 0a′−0a″ transition is shown just below as a red solid line. The simulated stick spectrum (lower trace) is obtained from the FC simulation (see the text). Dots and asterisks are denoted for "e' and 'a" symmetry species of the CH_3 internal rotor, respectively. The hindered rotor transitions are depicted according to the internal rotor quantum numbers (m) of S_0 (subscript) and S_1 (superscript). The out-of-plane dihedral torsional mode (τ) of the SCH_3 moiety with respect to the molecular plane is found to be activated (see the text). The R2PI bands due to the *trans* conformer are denoted as a solid blue line. (b) The sinusoidal model potential energy curve for the CH_3 internal rotor in S_0 (lower) shows the tunneling split when $F = 5.317_7$ (5.301$_6$) cm^{-1} and $V_3 = 27$ (300) cm^{-1} for S_0 (S_1). The double well potential energy curve ($V_{S_0} = (1/2)k'x^2$, $V_{S_1} = (1/2)\ k'x^2 + A' \exp(-a'x^2)$) along the out-of-plane dihedral torsional mode is depicted (upper) with associated eigenvalues (see the text). Parameters used are $k' = 0.0002419$ (0.00016) [hartree/a_0^2], reduced mass of 2.797 (2.998) [amu] for S_0 (S_1), $A' = 0.00058$ [hartree], and $a' = 0.667$ [a_0^2] for S_1. a_0 is the Bohr radius. Inset molecules are calculated (RICC2, aug-cc-pVDZ) (lower) as minimum energy S_0 structure and (upper) out-of-plane SCH_3 torsional vibrational normal-mode displacement, respectively.

energy of 4.1 cm^{-1}. The energetic gap of the split remains identical for all vibronic bands, indicating that the doublet originates from the a″−e″ split in the electronically ground state, also confirmed by the hole-burning spectroscopy, Figure 4. This rather large split of the doublet strongly suggests that the CH_3 torsional barrier in S_0 is very small, giving the estimation of ∼27 cm^{-1} for V_3 from the theoretical simulation as described above. Therefore, in contrast to the case of the

https://dx.doi.org/10.1021/acs.jpca.0c03452
J. Phys. Chem. A XXXX, XXX, XXX−XXX

trans conformer, the series of the CH_3 torsional mode is almost absent in the R2PI spectrum of *cis*. And yet, on the other hand, it is found that a specific low-frequency vibrational mode is highly activated in the R2PI spectrum of the *cis* conformer, giving similar patterns for all combined modes including the S_1-S_0 origin (Figure 1). This mode is most likely due to the out-of-plane torsional motion of the SCH_3 moiety with respect to the molecular plane. As this mode is the torsion regarding the dihedral angle between the plane containing the S-CH_3 bond axis and that of the phenyl moiety, the double-well potential in the form of $V_{S_1} = (1/2)\ k'x^2 + A'\ \exp(-a'x^2)$ is used to reproduce the experiment. Indeed, the experiment could be fit very well, giving the shape of the S_1 potential curve with calculated eigenvalues (Figure 4). As the SCH_3 dihedral angle with respect to the molecular plane is very critical in terms of the nonadiabatic dynamics in the conical intersection region, the experimental fact that the S_1 structure of the *cis*-3-MTA adopts the nonplanar geometry at its minimum energy suggests that the S-CH_3 predissociation dynamics of the *cis* conformer could be somewhat different from that of the *trans* conformer in terms of the overall nonadiabaticity of the reaction. Indeed, according to our calculation at the RICC2 level with the aug-cc-pVDZ basis set, the *cis*-3-MTA undergoes the planar-to-pseudoplanar structural change upon the S_1-S_0 transition. Namely, the SCH_3 moiety becomes out-of-plane with respect to the molecular plane in S_1 of *cis*, which is quite consistent with the spectroscopic evidence.

Ab initio calculations for the CH_3 torsional potential energy curve for *cis* and *trans* in both S_0 and S_1 support the experiment very nicely (Figure 5). The eclipsed or staggered geometry is predicted to be more stable in S_0 or S_1 of the *trans*-3-MTA, respectively. Although they do not exactly match with the estimated values from the experiment, the theoretical torsional barrier heights of 47 and 388 cm^{-1} calculated for S_0 and S_1, respectively, match extremely well with the experiment (*vide supra*). The calculation supports the experiment quite nicely also for the *cis* conformer. The CH_3 torsional barrier height is predicted to be 20 or 394 cm^{-1} for S_0 and S_1, respectively. As there is little structural change in terms of the CH_3 torsion upon the S_1-S_0 transition of *cis*, the barrier height in S_1 is hardly verified. And yet, the calculated barrier height in S_0 is quite consistent with the simulated value inferred from the split of the doublet in the R2PI spectrum of *cis* (*vide supra*).

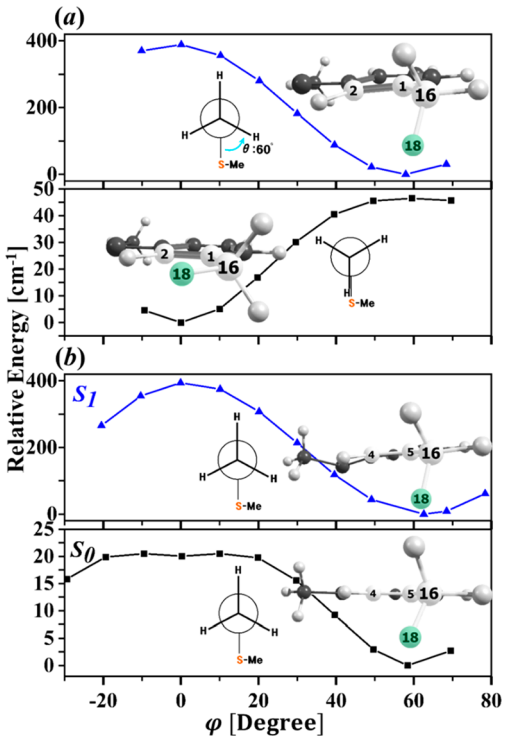

Figure 5. Potential energy curve with respect to the CH_3 torsional angle (φ) obtained by the relaxed scan for (a) *trans*-3-MTA and (b) *cis*-3-MTA. Insets show the calculated (RICC2, aug-cc-pVDZ) minimum energy structures with Newman projections.

CONCLUSIONS

Herein, the conformer-specific structural changes of 3-methylthioanisole upon the S_1 ($\pi\pi^*$)$-S_0$ excitation have been spectroscopically investigated. For the *trans* conformer, the methyl moiety on the meta-position undergoes the eclipsed-to-staggered geometrical change upon the S_1-S_0 transition, giving the 3-fold torsional barrier of 34 and 304 cm^{-1} for S_0 and S_1, respectively. For the *cis* conformer, the CH_3 torsion is little activated though the clearly resolved doublet of each vibronic band gives the very low torsional barrier of 27 cm^{-1} for the S_0 *cis* conformer. More interestingly, the *cis* conformer is found to be nonplanar in S_1 differently from S_0, implying that the S-CH_3 bond predissociation dynamics of *trans* and *cis* conformers of 3-methylthioanisole might differ in their nonadiabatic dynamic properties.

ASSOCIATED CONTENT

Supporting Information

The Supporting Information is available free of charge at https://pubs.acs.org/doi/10.1021/acs.jpca.0c03452.

Full R2PI with UV−UV hole-burning spectra, selective vibrational mode assignment, relaxed scan for torsional coordinate of methylthio moiety (−SCH_3), methyl-internal-rotation assignment (PDF)

AUTHOR INFORMATION

Corresponding Author

Sang Kyu Kim − *Department of Chemistry, KAIST, Daejeon 34141, Republic of Korea;* orcid.org/0000-0003-4803-1327; Email: sangkyukim@kaist.ac.kr

Authors

Heesung Lee − *Department of Chemistry, KAIST, Daejeon 34141, Republic of Korea;* orcid.org/0000-0001-7056-4053

So-Yeon Kim − *Department of Chemistry, KAIST, Daejeon 34141, Republic of Korea*

Jean Sun Lim − *Department of Chemistry, KAIST, Daejeon 34141, Republic of Korea*

Junggil Kim − *Department of Chemistry, KAIST, Daejeon 34141, Republic of Korea*

Complete contact information is available at: https://pubs.acs.org/10.1021/acs.jpca.0c03452

Notes

The authors declare no competing financial interest.

https://dx.doi.org/10.1021/acs.jpca.0c03452
J. Phys. Chem. A XXXX, XXX, XXX−XXX

■ ACKNOWLEDGMENTS

This work was supported by the National Research Foundation (NRF: 2018R1A2B3004534) and the Ministry of Education (2019R1A6A1A10073887) of Korea.

■ REFERENCES

(1) Parmenter, C. S.; Stone, B. M. The methyl rotor as an accelerating functional group for IVR. *J. Chem. Phys.* **1986**, *84* (8), 4710−4711.
(2) Moss, D. B.; Parmenter, C. S. Acceleration of intramolecular vibrational redistribution by methyl internal rotation. A chemical timing study of p-fluorotoluene and p-fluorotoluene-d_3. *J. Chem. Phys.* **1993**, *98* (9), 6897−6905.
(3) Timbers, P. J.; Parmenter, C. S.; Moss, D. B. Acceleration of intramolecular vibrational redistribution by methyl internal rotation. II. A comparison of m-fluorotoluene and p-fluorotoluene. *J. Chem. Phys.* **1994**, *100* (2), 1028−1034.
(4) Gascooke, J. R.; Lawrance, W. D. Methyl rotor dependent vibrational interactions in toluene. *J. Chem. Phys.* **2013**, *138* (13), 134302.
(5) Gardner, A. M.; Tuttle, W. D.; Whalley, L.; Claydon, A.; Carter, J. H.; Wright, T. G. Torsion and vibration-torsion levels of the S_1 and ground cation electronic states of para-fluorotoluene. *J. Chem. Phys.* **2016**, *145* (12), 124307.
(6) Tuttle, W. D.; Gardner, A. M.; Whalley, L. E.; Wright, T. G. Vibration and vibration-torsion levels of the S1 state of para-fluorotoluene in the 580−830 cm^{-1} range: Interactions and coincidences. *J. Chem. Phys.* **2017**, *146* (24), 244310.
(7) Ichimura, T.; Suzuki, T. Photophysics and photochemical dynamics of methylanisole molecules in a supersonic jet. *J. Photochem. Photobiol., C* **2000**, *1* (1), 79−107.
(8) Kinoshita, S.-i.; Kojima, H.; Suzuki, T.; Ichimura, T.; Yoshida, K.; Sakai, M.; Fujii, M. Pulsed field ionization zero kinetic energy photoelectron study on methylanisole molecules in a supersonic jet. *Phys. Chem. Chem. Phys.* **2000**, *3* (22), 4889−4897.
(9) Tardy, D. C.; Rabinovitch, B. S. Intermolecular vibrational energy transfer in thermal unimolecular systems. *Chem. Rev.* **1977**, *77* (3), 369−408.
(10) Nesbitt, D. J.; Field, R. W. Vibrational Energy Flow in Highly Excited Molecules: Role of Intramolecular Vibrational Redistribution. *J. Phys. Chem.* **1996**, *100* (31), 12735−12756.
(11) Boyall, D.; Reid, K. L. Modern studies of intramolecular vibrational energy redistribution. *Chem. Soc. Rev.* **1997**, *26* (3), 223−232.
(12) Lim, J. S.; Kim, S. K. Experimental probing of conical intersection dynamics in the photodissociation of thioanisole. *Nat. Chem.* **2010**, *2* (8), 627−632.
(13) You, H. S.; Han, S.; Yoon, J.-H.; Lim, J. S.; Lee, J.; Kim, S.-Y.; Ahn, D.-S.; Lim, J. S.; Kim, S. K. Structure and dynamic role of conical intersections in the $\pi\sigma^*$-mediated photodissociation reactions. *Int. Rev. Phys. Chem.* **2015**, *34* (3), 429−459.
(14) Woo, K. C.; Kang, D. H.; Kim, S. K. Real-Time Observation of Nonadiabatic Bifurcation Dynamics at a Conical Intersection. *J. Am. Chem. Soc.* **2017**, *139* (47), 17152−17158.
(15) Han, S.; Lim, J. S.; Yoon, J.-H.; Lee, J.; Kim, S.-Y.; Kim, S. K. Conical intersection seam and bound resonances embedded in continuum observed in the photodissociation of thioanisole-d_3. *J. Chem. Phys.* **2014**, *140*, 054307.
(16) Lee, J.; Kim, S.-Y.; Kim, S. K. Spectroscopic Separation of the Methyl Internal-Rotational Isomers of Thioanisole Isotopomers (C_6H_5S-CH_2D and C_6H_5S-CHD_2). *J. Phys. Chem. A* **2014**, *118* (10), 1850−1857.
(17) Kim, S.-Y.; Lee, J.; Kim, S. K. Conformer specific nonadiabatic reaction dynamics in the photodissociation of partially deuterated thioanisoles (C_6H_5S-CH_2D and C_6H_5S-CHD_2). *Phys. Chem. Chem. Phys.* **2017**, *19* (29), 18902−18912.
(18) Lim, J. S.; You, H. S.; Kim, S.-Y.; Kim, S. K. Experimental observation of nonadiabatic bifurcation dynamics at resonances in the continuum. *Chem. Sci.* **2019**, *10* (8), 2404−2412.
(19) Frisch, M. J.; Trucks, G. W.; Schlegel, H. B.; Scuseria, G. E.; Robb, M. A.; Cheeseman, J. R.; Scalmani, G.; Barone, V.; Mennucci, B.; Petersson, G. A.; Nakatsuji, H.; Caricato, M.; Li, X.; Hratchian, H. P.; Izmaylov, A. F.; Bloino, J.; Zheng, G.; Sonnenberg, J. L.; Hada, M.; Ehara, M.; Toyota, K.; Fukuda, R.; Hasegawa, J.; Ishida, M.; Nakajima, T.; Honda, Y.; Kitao, O.; Nakai, H.; Vreven, T.; Montgomery, J. A., Jr.; Peralta, J. E.; Ogliaro, F.; Bearpark, M.; Heyd, J. J.; Brothers, E.; Kudin, K. N.; Staroverov, V. N.; Kobayashi, R.; Normand, J.; Raghavachari, K.; Rendell, A.; Burant, J. C.; Iyengar, S. S.; Tomasi, J.; Cossi, M.; Rega, N.; Millam, J. M.; Klene, M.; Knox, J. E.; Cross, J. B.; Bakken, V.; Adamo, C.; Jaramillo, J.; Gomperts, R.; Stratmann, R. E.; Yazyev, O.; Austin, A. J.; Cammi, R.; Pomelli, C.; Ochterski, J. W.; Martin, R. L.; Morokuma, K.; Zakrzewski, V. G.; Voth, G. A.; Salvador, P.; Dannenberg, J. J.; Dapprich, S.; Daniels, A. D.; Farkas, O.; Foresman, J. B.; Ortiz, J. V.; Cioslowski, J.; Fox, D. J. *Gaussian 09*, revision A.1; Gaussian, Inc.: Wallingford, CT, 2009.
(20) *Turbomole, a development of University of Karlsruhe and Forschungszentrum Karlsruhe GmbH*, V7.0.2; Turbomole GmbH, 2015, http://www.turbomole.com.
(21) You, H. S.; Kim, J.; Han, S.; Ahn, D.-S.; Lim, J. S.; Kim, S. K. Spatial Isolation of Conformational Isomers of Hydroquinone and Its Water Cluster Using the Stark Deflector. *J. Phys. Chem. A* **2018**, *122* (5), 1194−1199.
(22) Chang, Y.-P.; Horke, D. A.; Trippel, S.; Küpper, J. Spatially-controlled complex molecules and their applications. *Int. Rev. Phys. Chem.* **2015**, *34* (4), 557−590.
(23) Chang, Y.-P.; Filsinger, F.; Sartakov, B. G.; Küpper, J. CMIstark: Python package for the Stark-effect calculation and symmetry classification of linear, symmetric and asymmetric top wavefunctions in dc electric fields. *Comput. Phys. Commun.* **2014**, *185* (1), 339−349.

https://dx.doi.org/10.1021/acs.jpca.0c03452
J. Phys. Chem. A XXXX, XXX, XXX−XXX